2018 Spring Technical Meeting
Central States Section of The Combustion Institute
May 20–22, 2018
Minneapolis, Minnesota

Chemiluminescence measurements in a combustor using a 7-point lean direct injector array configuration for gas turbine engine applications

Tyler G. Capil[1], Kathleen M. Tacina[1], Yolanda R. Hicks[1]*

[1]NASA Glenn Research Center, Cleveland, Ohio, USA
[*]Corresponding Author Email: tyler.g.capil@nasa.gov

Abstract: Two different configurations of a 7-point lean direct injector array were investigated. Chemiluminescence images of C_2* or CH* were collected during combustion tests for insight on flame structure for the two configurations. Several inlet conditions were tested by varying the equivalence ratio or reference velocity. For the center right-hand 60˚ and outer right-hand 52˚ outers, the chemiluminescence emanating from the central pilot appeared well isolated from the outers. At the same time, a hollow region below the pilot showed little fluctuation of chemiluminescence where a central recirculation zone was present during the non-reacting tests. The central left-hand 60 and outer right-hand 52˚ configuration displayed a narrower structure from the pilot compared to the flatter pilot observed in the other configuration. Additionally, the right-handed outer swirlers may be responsible for the asymmetry observed with the chemiluminescence images. Both configurations showed less variation in chemiluminescence intensity as the reference velocity was increased. This was likely due to better atomization and vaporization associated with higher fuel and air flow rates.
Keywords: lean direct injection, chemiluminescence, gas turbine engine

1. Introduction

This paper presents results from combustion tests using a 7-point lean direct injector array to observe fuel-air mixing by changing the center pilot swirl angle. Previously, a parametric study for non-reacting flows as well as Jet-A/air reacting flows from reference [1,2] covered several air swirler configurations for the 7-point LDI module. The parameter study included changes to center pilot offset and air swirl angle. Non-reacting tests examined the formation or absence of a central recirculation zone. This was achieved by examining water spray through the nozzle through particle image velocimetry. The non-reacting cases in reference [2] found that the close spacing between elements in the 7-point array caused significant element-to-element interactions that determined the formation of a central recirculation zone. Furthermore, those studies indicated that recessing the center pilot or using counter-swirlers resulted in better isolation among other swirlers.

The premise of this paper explores combustion tests with Jet-A/air for two different configurations of the 7-point LDI array. Primarily, the objective was to study flame structure between the two configurations through chemiluminescence imaging. An additional layer of comparison was presented to examine the effects of equivalence and reference velocity. A brief discussion of cold-flow PIV results was included.

2. Methods / Experimental

2.1 LDI Configuration

From Figure 1a, the swirl-venturi LDI consists of axial air swirlers to allow air passage into the converging-diverging venturi. Seven of the single elements are placed in an array to form the 7-point LDI array shown in Figure 1b. Each air swirler is six-bladed with a hub diameter of 0.34-in and a blade diameter of 0.8725-in. The fuel injector is positioned through the hub of the axial swirler and the tip of the injector is placed at the venturi throat. The venturi has a diameter of 0.5-in with a throat length of 0.061-in. Lastly, the fuel injector is a simplex nozzle that creates a hollow cone with a spray angle of 70˚; the flow number FN_{US} is roughly 0.70.

(a) (b)

Figure 1: (a) Detailed illustration of a single LDI element. (b) Schematic of 7-point LDI array

Two configurations of the 7-point, shown in Figure 1b, were investigated in this paper. The first configuration, namely Configuration 1, consisted of a right-hand 60˚ center pilot swirler and right-hand 52˚ on the six outer swirlers. The second configuration, namely Configuration 2, used a left-hand 60˚ center pilot swirler and maintained the right-hand 52˚ on the outers.

2.2 Test Facility

Testing conducted in the Combustion and Dynamics Facility (CDF). THE CDF supplies non-vitiated air where flow through the combustor is top to bottom. Preheated air enters the combustor capable of reaching temperatures of up to 810 K, air flow rates up to 0.35 lbm/s, and pressures up to 517 kPa. The combustor section consists of a circular cross-section with a 7.68-in nominal diameter. As shown in Figure 2a, three sets of double-paned windows are arranged circumferentially around the combustor 90˚ apart. Windows are flat and are positioned offset to the combustor cross-section. These windows provide optical access into the combustor. The dimensions of the windows are 6.1-cm tall and 5.8-cm wide.

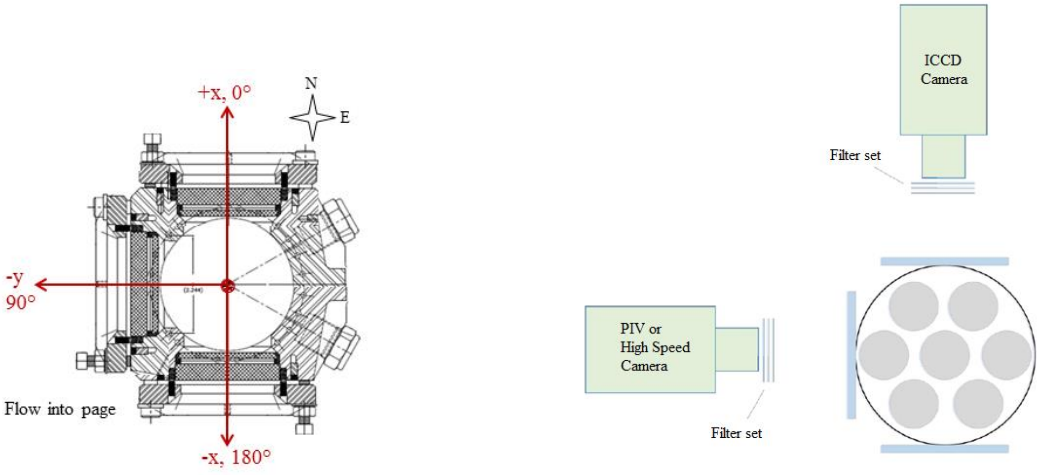

(a) (b)

Figure 2: (a) Schematic of combustor shows orientation of windows and establishes coordinate system. (b) Sketch showing orientation of ICCD camera relative to 7-point array.

2.3 Optical Instrumentation and Test Conditions

Chemiluminescence images of C_2^* and CH^* were acquired with a gated, 16-bit, 1k x 1k pixel array, intensified CCD (ICCD) camera. The orientation of the ICCD camera relative to the 7-point array is shown in Figure 2b. Images were collected with a 500 ns gate at a frame rate of 25 Hz. Chemiluminescence imaging is a volume-based, line-of-sight integrated measurement of radical combustion species and does not isolate individual planes. However, chemiluminescence imaging of C_2^* and CH^* were still useful to image because their concentrations are generally near locations of peak heat release. In addition, C_2^* and CH^* indicated the areas of the primary reaction zone where the carbon-carbon and carbon-hydrogen species breakdown. Narrow bandwidth filters were coupled with the ICCD in order to spectrally isolate C_2^* and CH^* signals. C_2^* was captured with a 515 nm filter (FWHM 12 nm). Similarly, CH^* was isolated with a 430 nm filter (FWHM 11 nm).

Cold-flow testing was done to observe the flow field by examining water spray through the nozzle using PIV. The non-reacting tests were completed for each configuration where configuration 1 was studied in reference [2], and a brief discussion of configuration 2 was included in this paper. The PIV was performed by creating a laser sheet aligned along the y-z plane using a set of cylindrical lenses. A 15-Hz, dual head, frequency-doubled, Nd:YAG laser was used to scatter light off of water spray through the nozzle. The scattered light was captured by an interline transfer, CCD camera which was positioned as shown in Figure 2b. The laser sheet was moved in 1-mm increments along the y-coordinate where 500 images pairs were collected per location. DaVis version 8.1.2 software was used to analyze the PIV data through multi-pass cross-correlation vector processing.

Table 1 shows six inlet conditions were considered in this study to examine the effects of varying equivalence ratio and reference velocity. All conditions were tested with an inlet pressure of 75 psia and an inlet temperature of 800 ˚F.

The first three points provided a comparison on equivalence ratios of 0.450, 0.480, and 0.500, respectively where the pilot and outers had equal fuel staging. The conditions in the first and last row of Table 1 examined the effect of reference velocity. The center pilot and outer equivalence ratios were kept at 0.450. However, one inlet condition had a reference velocity of 40 ft/s and the other condition had a reference velocity of 35 ft/s.

Table 1: Inlet conditions tested for the 7-point LDI configurations

P_3 psia	T_3 ˚F	u ft/s	Φ	Φ_c	Φ_o
75	800	35	0.450	0.450	0.450
75	800	35	0.480	0.480	0.480
75	800	35	0.500	0.500	0.500
75	800	40	0.450	0.450	0.450

3. Results and Discussion

In this paper, the statistical results were processed for individual chemiluminescence species over 500 images. The root-mean-square (RMS) was chosen over the average in order to remove noise averaged in camera read-out, blackbody radiation, and etc. The noise within the averages resulted in distorted interpretations. RMS helped by subtracting out the mean extraneous signal, leaving the relevant signal. Furthermore, the RMS indicated the flame structure by illustrating the fluctuations in the chemiluminescence signal.

3.1 Configuration 1: Co-rotating, right-hand 60˚ center, right-hand 52˚ outer

Figure 6 shows the RMS of the CH^* signals for configuration 1. The highest variations in the chemiluminescence emerged out of the center pilot, and the outer flames can be seen at the sides of the field-of-view. In the center region directly downstream of the pilot, smaller fluctuations in CH^* were found. Reference [2] presented a cold-flow analysis for this particular configuration. It is interesting to note that the area of weak chemiluminescence signal observed in the reacting cases shared a similar shape to that of the central recirculation zone in the cold-flow cases.

Left to right the equivalence ratio increases from 0.450, 0.480, and 0.500. As the conditions became richer, the variations in CH^* become larger and extended further downstream. This makes sense as richer mixtures lead to more abundance of free radicals. At the same time, the signals that were found further downstream indicated the longer flame length as equivalence ratio increased.

A comparison of two different reference velocity conditions is presented in Figure 4, where the left and right images show reference velocities of 35 ft/s and 40 ft/s respectively. The chemiluminescence presented was of C_2^*, which appeared to have stronger signal compared to CH^*. Overall, the flame structure had the familiar chemiluminescence that emanated from the

center pilot near the dome and downstream signals that originated from the outers. Increasing the reference velocity from 35 ft/s to 40 ft/s resulted in a similar flame structure. However, the RMS of C_2^* was smaller for the higher reference velocity condition. This was possibly due to the differences in atomization. With higher air flow rates, the interaction between the fuel spray and surrounding air resulted in enhanced disintegration of the fuel into droplets. Additionally the fuel flow rate had to be increased to accommodate the same equivalence ratio. According to [3] the increase in pressure drop across the nozzle, and therefore increase in flow rate, increases the atomization and fuel distribution processes. With better atomization, the fuel droplets vaporize more effectively. As a result, the chemiluminescence signals appeared weaker.

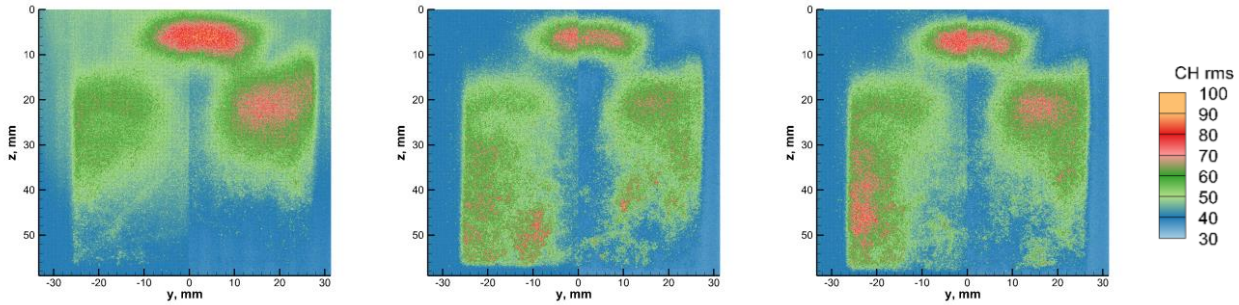

Figure 3. RMS of CH^* for configuration 1. Left to right the equivalence ratios were 0.450, 0.480, and 0.500.

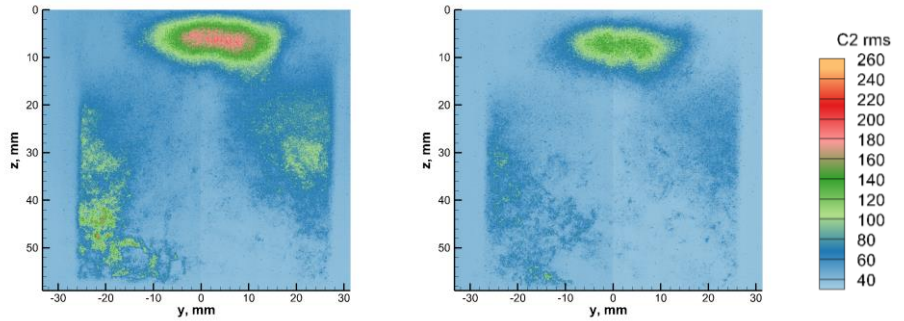

Figure 4. RMS of C_2^* for configuration 1. Reference velocities of 35 ft/s (left) and 40 ft/s (right).

3.2 Configuration 2: counter-rotating, left-hand 60° center, right-hand 52° outer

The average velocity vectors for configuration 2 are shown in Figure 5 at three different y-positions. These results were tested with a reference velocity of 50 ft/s. In the center plane at y = 0, there was a slower patch of moving air which hinted at a central recirculation zone. At y = -12 mm and y = 12 mm, the central recirculation zone disappeared and much of the flow field downstream of the dome showed movement in the right-handed direction.

Figure 6 shows CH^* results of the counter-rotating configuration. Equivalence ratios varied from left to right at 0.450, 0.480, and 0.500. Similar to configuration 1, increasing the equivalence ratio resulted in fluctuations in CH^* to extend farther downstream and overall higher variations in CH^*. The flame structure implied by the chemiluminescence for the counter-rotating configuration was noticeably different compared to co-rotating case. One thing to note from the counter-rotating case was the shape emerging from the pilot, which had a more triangular shape

compared to the round, flat shape observed in configuration 1. This narrower shape was also similar to the shape of the slower patch of air seen from the PIV results. Another characteristic of the chemiluminescence showed CH^* RMS concentrated towards the right-hand portion of the images. The asymmetry of the chemiluminescence is still under speculation; however, it may be possible that the downstream swirl caused stronger signals on the side of the image approaching the camera and weaker signals on the part of the image away from the camera.

The C_2^* chemiluminescence results for changes in reference velocity from configuration 2 are shown in Figure 7. As previously observed with the co-rotating case, the counter-rotating configuration showed a decrease in C_2^* RMS as the reference velocity increased. With the better atomization and fuel distribution associated with higher air and fuel flow rates, the C_2^* RMS varied less for the higher reference velocity. The weaker chemiluminescence comes as a result of improved fuel vaporization.

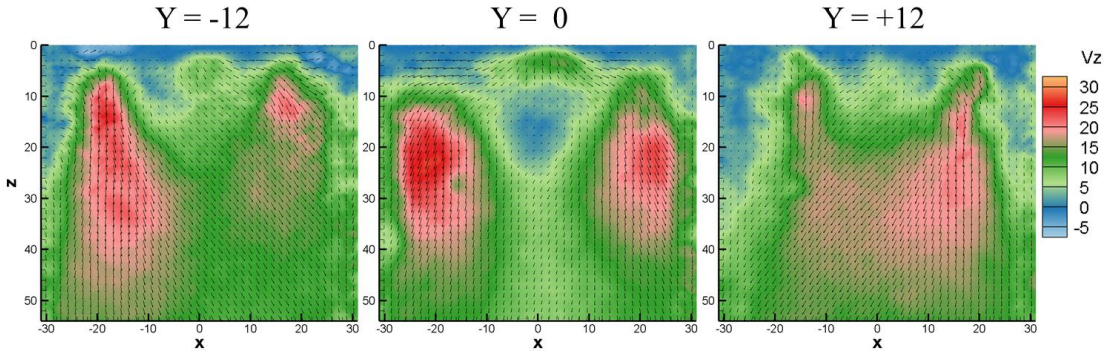

Figure 5. Non-reacting results from PIV showing average velocity vectors at positions y = -12 mm, y = 0 mm, and y = 12 mm. Reference velocity for this condition was 50 ft/s.

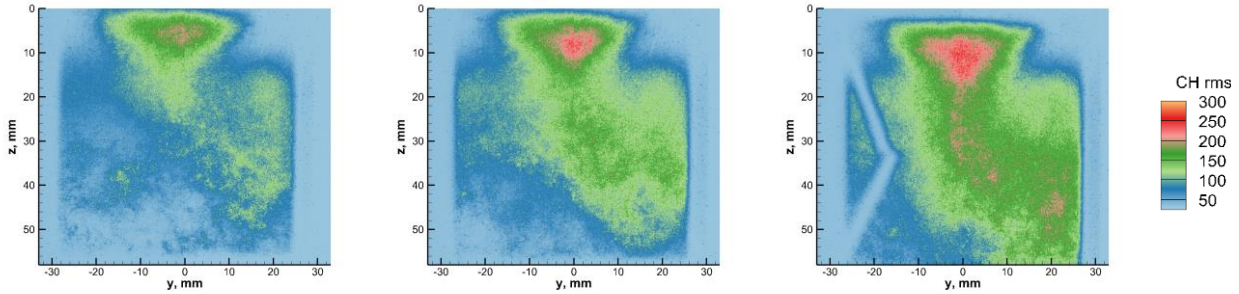

Figure 6. RMS of the CH^* signal for configuration 2. Left to right the equivalence ratios were 0.450, 0.480, and 0.500 respectively.

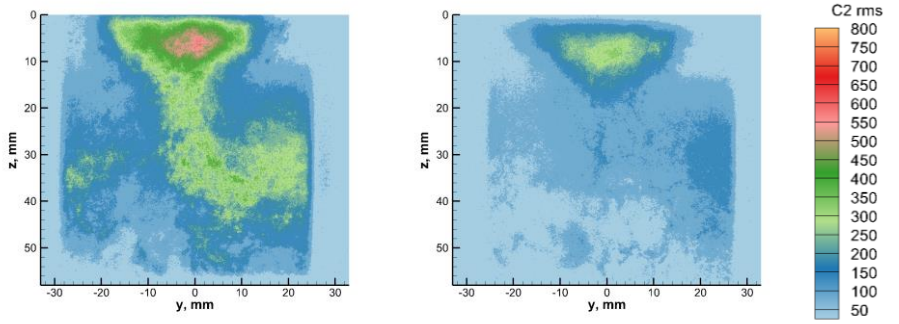

Figure 7. Root-mean-square of C_2^* signal from configuration 2 for reference velocities of 35 ft/s (left) and 40 ft/s (right).

4. Conclusions

Chemiluminescence results were presented for two LDI configurations under varying equivalence ratios and reference velocities. The right-hand 60˚ center and right-hand 52˚ outer configuration showed a flat, round shaped pilot. The outer flames were separated by a region of weaker chemiluminescence in line with the center of the injector, which seemed to coincide with the long recirculation zone seen in previous cold-flow testing. In contrast, the left-hand 60˚ center and right-hand 52˚ outer case showed a tornado-like pilot. Much of the chemiluminescence fluctuation appeared right-handed, which could be due to dominance of the right-hand swirl further downstream. For both configurations, the increased equivalence ratio resulted in observed longer flame lengths as well as larger fluctuations in chemiluminescence intensity. Additionally, the increased reference velocity for both configurations resulted in a decrease in RMS chemiluminescence. This decrease may be due to the smaller fuel drop sizes and distribution of fuel associated with higher fuel and air flow rates.

Future additional work includes cold-flow and combustion testing for other configurations of this hardware. Plans for testing a new design of the 7-point LDI hardware by Woodward will follow.

5. Acknowledgements

This work was supported by the Transformational Tools and Technologies Project under the NASA Aeronautics Research Mission Directorate.

6. References

[1] Y.R. Hicks, K.M. Tacina, R.C. Anderson, S.A. Tedder, A comparison of Flow Fields Generated by Varying Air Swirler Configurations in a 7-Point Lean Direct Injector Array, 2016 Spring Technical Meeting, Central States Section of the Combustion Institute, 2016.

[2] Y.R. Hicks, K.M. Tacina, R.C. Anderson, Effect of Air Swirler Configuration on Lean Direct Injector Flow Structure and Combustion Performance with a 7-point Lean Direct Injector Array, ISABE-2017-22620, 2017.

[3] A.H. Lefebvre, *Gas Turbine Combustion*. Taylor and Francis. Ann Arbor, U.S.A., 1998.